Acta Societatis Botanicorum Poloniae

ORIGINAL RESEARCH PAPER Acta Soc Bot Pol 84(3):369–383 DOI: 10.5586/asbp.2015.027
Received: 2014-12-30 Accepted: 2015-06-15 Published electronically: 2015-10-07

Quantifiable differences between phytolith assemblages detected at species level: analysis of the leaves of nine *Poa* species (Poaceae)

Zsuzsa Lisztes-Szabó[1]*, Szilvia Kovács[1], Péter Balogh[2], Lajos Daróczi[3], Károly Penksza[4], Ákos Pető[5]

[1] Department of Agricultural Botany, Crop Physiology and Biotechnology, University of Debrecen, Böszörményi u. 138, 4032 Debrecen, Hungary

[2] Department of Economic Analytical Methodology and Statistics, University of Debrecen, Böszörményi u. 138, 4032 Debrecen, Hungary

[3] Department of Solid State Physics, University of Debrecen, Egyetem tér 1, 4032 Debrecen, Hungary

[4] Department of Botany, Szent István University, Páter Károly u. 1, 2100 Gödöllő, Hungary

[5] Institute of Nature Conservation and Landscape Management, Szent István University, Páter K. u. 1, 2100 Gödöllő, Hungary

Abstract

The taxonomic value of phytolith assemblages and their degree of variability within different species of the same genus is still an undervalued issue in the botanical range of phytolith studies. However the understanding of grass phytolith variance and its implications to plant systematics is doubtless.

In the present study phytoliths of the lateral shoots (leaves) of nine, globally distributed *Poa* species (Pooideae – Poaceae) are described. Phytoliths were recovered from *Poa* specimens by the dry ashing technique. Altogether 6223 disarticulated phytoliths were counted (approximately 500–700 phytoliths per species) in 54 plant samples, which cover six shoots of nine species. Not only the relative frequency of each morphotype was calculated, but measurements were conducted to determine the biogenic silica content of *Poa* lateral shoots. A phytolith reference collection for the nine selected species of a worldwide importance was also compiled. The description of the most significant phytolith morphotypes and their taxonomic relationships are given here.

Results suggest that the biogenic silica content of the *Poa* lateral shoots was determined to be relatively high within all nine species. Phytolith assemblage data was subjected to multivariate statistical analyses (e.g., CA and PCA) in order to find differences and similarities among the nine *Poa* species. Results show that the two closely related *Poa* of the *P. pratensis* species group, namely the *P. pratensis* and *P. angustifolia*, only slightly differ from the other *Poa* species if we consider their rondel-trapeziform short cells (SC) phytolith frequencies.

Keywords: biogenic silica; epidermis; phytolith assemblage; *Poa*; silica bodies

Introduction

Many plants deposit hydrated SiO_2 in cell walls, cells and characteristic structures in intercellulars (silica bodies, phytoliths) [1,2]. Several studies link phytolith morphotypes to plant families and subfamilies (in Poaceae) [3–8]. In addition, it has been shown that there is a correlation between phytolith morphotypes and the C3 and C4 photosynthetic pathways and this allows the reconstruction of plant communities and climate through time [7,8]. It seems though that the phenotypic plasticity of phytoliths induced by environmental changes cannot entirely hide the potential of phytolith morphometries in discriminating plant taxa. Some cases are known in which the phytolith shapes of plant reference material allowed the correct identification to species level [9]. For example Mejia-Saules and Bisby [10] found distinguishing silica bodies in the lemmae of *Melica* species. Form and position of phytoliths, which are not greatly influenced by environmental factors but are genetically controlled, may have considerable systematic potential [11–13].

With approximately 500 species, the meadow-grass genus *Poa* L. is the largest genus in the Poaceae [14], and *Poa* species are common in the Northern Hemisphere. The genus includes important turf and forage grasses (*Arrhenatheretea*) [15,16] and cultivars as well as troublesome weeds and invaders [14,17]. Although primarily found in the temperate zone, *Poa* is a very widely distributed grass genus [18]. Blinnikov et al. [19] used *Poa* phytoliths alongside *Stipa* and *Festuca* in the identification of vegetation composition in the Columbia basin. Regarding the *Poa* genus, the *Poa pratensis* L. species group [*P. alpigena* (Fries) Lindman, *P. pratensis* L., *P. angustifolia* L.] [20] is one of the taxonomically most complicated groups in the

* Corresponding author. Email: szabozs@agr.unideb.hu

Handling Editor: Elżbieta Bednarska-Kozakiewicz

This is an Open Access article distributed under the terms of the Creative Commons Attribution 3.0 License (creativecommons.org/licenses/by/3.0/), which permits redistribution, commercial and non-commercial, provided that the article is properly cited. © The Author(s) 2015 Published by Polish Botanical Society

world. *Poa stiriaca* Fritsch et Hayek can also be classified in this group [15]. The features of the leaf epidermis, and the presence and distribution of silicified unicellular hairs and prickles were shown to be useful characteristics to separate and identify the species of the *P. pratensis* species group [21–24]. Nevertheless *P. pratensis* was often used as a "model" organism in many studies [25].

The aim of this study is to describe the phytolith assemblage in lateral shoots of nine *Poa* species, looking for potential species level phytolith characters that could be useful in palaeocecology and, in parallel, to start collecting reference material to make comparisons with other grass species and genera.

Material and methods

Sample collections

The following *Poa* species from the *P. pratensis* group were collected and analyzed: *P. alpigena* (Fries) Lindman, *P. angustifolia* L., *P. pratensis* L., and *P. stiriaca* Fritsch et Hayek. Other selected species consisted of two annual taxons: *P. annua* L., *P. compressa* L., *P. trivialis* L. and three perennial taxons: *P. arctica* R. Br. and *P. hybrida* Gaudich. The individuals of the species that were selected to be studied are characterized by wide geographical distribution. Most of the plant material originated from caryopses of the nine species obtained from the National Germplasm System of the United States Department of Agriculture [26] *Poa* collection. They were established in a climate room then planted into experimental plots under the same conditions. The studied germplasm were selected from different countries, with large geographical variation to represent different genetic backgrounds (Tab. 1). Proper identification of the grown specimen were undertaken in order to analyse relevant phytolith morphologies. A smaller part of plant material was collected at Hungarian localities (Tab. 1), except the specimens of *P. arctica*, *P. alpigena* and *P. hybrida*, because of the areas of these species do not reach the Carpathian basin (Tab. 1).

Laboratory procedures and data analysis

Six lateral shoots (leaf blades and leaf sheaths) of each species were compounded and treated as one single sample. Phytolith extraction and biogenic silica content (bSi) measurements were accomplished through the dry-ashing technique based on the methodological guidelines published by Albert and Weiner [27] and Mercader et al. [28,29]. The ashes were mixed thoroughly, then mounted on light microscope slides in immersion oil and observed with a Zeiss Axioskop 2+ microscope at a magnification of 1000×. 500–600 pieces of identifiable plant opal particles – phytoliths – per species were counted in adjacent but not in overlapping lines across the cover slip (with 22 mm length). Their morphological classification was accomplished based on Twiss et al. [3], whilst the denomination of individual morphotypes was accomplished according to the International Code for Phytolith Nomenclature 1.0 (ICPN 1.0 [30]). The classification and nomenclature work was complemented with the system of other authors (e.g., [16,28,31–34]). Meanwhile we documented the phytolith morphotypes by taking microphotographs. The frequency of individual morphotypes was calculated and the results visualized with the help of C2 ecological data visualization software [35]. The ubiquity of morphotypes was noted. Correlations between classified phytolith number and biogenic silica content were determined using the Pearson correlation coefficient. Hierarchical cluster analysis based on phytolith assemblages was used to estimate taxonomic value of phytolith morphotypes in the species. The dissimilarity coefficient was Euclidean distance and sorting strategy was single link [36]. To establish the degree of segregation of species based on phytolith morphotypes and to analyze the importance of morphotypes in this segregation, principal component analysis (PCA) was performed using SPSS 15.0 for Windows (SPSS, Chicago, IL, USA).

The adaxial and abaxial epidermis of three, dried leaves from three different lateral shoot per species were studied using AMRAY 1830I type scanning electron microscope (SEM). To illustrate the locality of the phytoliths in the epidermis tissue black scatter SEM images were made on *P. pratensis* and *P. angustifolia* leaves surfaces.

Tab. 1 Inventory of the examined *Poa* species and their biogenic silica content expressed in the plant's dry weight.

Number	Species	Original locality	Biogenic silica (%)	Leaf width (mm)
1	*P. pratensis*	Iran, Hungary	12.0	2.0–4.0
2	*P. angustifolia*	China, Hungary	22.8	0.5–1.0#
3	*P. alpigena*	Alaska, Norway	29.2	0.9–1.3*
4	*P. stiriaca*	Poland, Hungary	22.0	0.2–0.3
5	*P. annua*	India, Hungary	16.0	1.0–5.0
6	*P. arctica*	Canada, Alaska	7.1	1.0–2.5
7	*P. compressa*	Russia, Hungary	15.1	1.0–4.0
8	*P. hybrida*	USA, Canada	12.6	5.0–8.0
9	*P. trivialis*	Morocco, Hungary	14.7	1.5–6.0

Leaf width data are based on [14], #[15], *[51].

Results

Biogenic silica content

The ash of the *Poa* shoots contained fully silicified silica bodies, cells with silicified walls, corroded silicified cells and debris of silicified cell walls and parts of the epidermis tissue. The average silica content was 16.8% of the plant's dry weight (range: 7.1% of *P. arctica* and 29.2% of *P. alpigena*) in the *Poa* shoots (Tab. 1). There may be some correlation between the bSi content and width of the leaves of the studied species because the higher bSi content was coupled with narrower leaves, but the negative correlation is not significant ($r = -0.45$; $P = 0.22$).

Descriptive results of lateral shoots phytoliths in *Poa* species

Approximately 300–1000 microphotographs were taken of every species with a total of 2703 (66–855 per species) showing classified and a total of 3520 (82–1243 per species) showing unclassified phytoliths. Altogether 6223 phytoliths were counted. Some (142) tissue microphotographs were taken because the cells strongly adhered to each other in the ash (cf. silica sheet elements). Altogether 31 morphotypes are reviewed in this study. This includes those two morphotypes, which are considered to be new [24], because they may bear taxonomical properties.

Classified phytoliths

An average of 76.8% of the nine *Poa* species phytoliths were identifiable as an established morphotypes (Tab. 2). In *P. angustifolia*, *P. stiriaca*, and *P. hybrida* the percentage of classified phytoliths exceeded 60% and in *P. compressa* it was 50%. This value was below 50% in *P. trivialis*, under 30% in *P. alpigena* and *P. annua*, and little more than 30% in *P. arctica*. *Poa angustifolia* had more classified phytoliths and biogenic silica content than the close relative *P. pratensis* with wider leaves. We did not find correlation between classified phytolith number and biogenic silica content ($r = 0.128$; $P = 0.742$).

Tab. 2 and Fig. 1–Fig. 5 give a summary of the relative frequencies and observed features of phytolith assemblages of *Poa* shoots. The phytolith assemblage of the nine examined *Poa* species leaves were characterized by elongate psilate proportion above 45%, elongate sinuate proportion above 10% and proportion of rondel trapeziform above 20%. Globular, tabular and lanceolate phytoliths were below 5% (Fig. 1).

Phytoliths with high frequency values (above 20%)

The anatomical origin of most of the phytolith morphotypes is the epidermis, as is usual in the Poaceae family. The elongate long cells (LC) and short cells (SC) were common in these species. Elongate morphotypes could be observed with several textures and ornamentation types. The number of ornamentation types varied between two and ten. *Poa hybrida* and *P. alpigena* had two elongate ornamentation types, whilst *P. pratensis* showed ten different ornamentation types (Tab. 2). The most common ornamentation types are psilate and sinuate textures, and these can be found in every species. Elongate echinate morphotypes are also common and can be found in leaves of six species. Some of the elongate psilate morphotypes derive from the vascular system (Fig. 4). The elongate depressed psilate morphotype could be found in five species at low frequency, seeming to be a peculiarity of *Poa* species [24].

The rondel-trapeziform morphotype (short cells of the epidermis) was common in *Poa* species and frequent in *P. pratensis* (32.4%) and *P. angustifolia* (55.9%) leaves. Rondel-trapeziform short cells were similar in frequency in *P. annua* (17.8%), *P. alpina* (17.5%) and *P. hybrida* (15.7%), but other species had rather less rondel.

Phytoliths with low frequency values (below 20%)

Globular psilate forms with inclusion occurred in leaves of *P. alpigena*, *P. arctica* and of *P. compressa* at high frequency. These phytoliths are presumably mesophyll cells with more or less regular, square inclusions in them. These small square inclusions can also be found in the ash in free state.

Lanceolate trichomes were seen in every species with the exception of *P. alpigena*. Lanceolate trichomes and bulliforms were in low abundance in this species, the frequencies of trichomes were 0–4.8% and bulliforms were 0–2.8%. Papillae (silicified prickles with rounded ends) were seen only in the leaves of *P. pratensis*. The trigonal pyramid morphotype was described in *P. pratensis* individuals [24] and it was found in *P. angustifolia* and *P. arctica* leaves at low frequency. Papillae with pitted edges could be found only in *P. compressa* with a frequency of 0.2%. The lobate morphotypes are not so typical in the studied *Poa* species (polylobate: 0.1%, bilobate: 0.03%).

Differencies of phytolith assemblages among the nine *Poa* species

Scanning electron microscope images (Fig. 6–Fig. 9) illustrate the phytolith assemblage of the species summarized in Fig. 1. At every species, the adaxial surfaces contain trichomes (prickles) without distinguishable costal zones and silicified short cells. The abaxial surfaces contain distinguishable costal and intercostal zones and costal zones may be abundant in silicified short cells. *Poa pratensis* (Fig. 6a,b) and *P. angustifolia* (Fig. 6c,d) back scatter SEM images show the locality of the phytoliths in both of the leaf surfaces by the lighter silica bodies. The adaxial epidermis produce more silicified long cells (and trichomes) than the abaxial surfaces. Stomata are not silicified. The leaf epidermis of *P. pratensis* can be characterized by abundant rondel-trapeziform SC and lanceolate unicellular trichome (or short prickle) phytoliths. The adaxial surfaces produced more trichomes and elongate LC morphotypes than the abaxial surfaces (Fig. 7a,b). Epidermis surfaces of *P. angustifolia* leaves are similar to those of *P. pratensis* but costal zones are wider with more cell rows than the costal zone of adaxial epidermis of *P. pratensis* leaves (Fig. 7c,d). Silification of short cells was not so typical in *P. alpigena* epidermis (embedded picture in Fig. 7e,f), but globular inclusion and small square phytoliths were observed in bigger amounts (Fig. 1). *Poa stiriaca* was characterized by abundant elongate LC, specially high elongate castelate LC, and the least rondel-trapeziform SC among the studied *Poa* species (Fig. 8a,b). *Poa annua* is characterized by rectangulare phytoliths, but prickles were not found to be typical for this species (Fig. 8c,d). *Poa arctica* leaves produced more globular morphotypes than the other studied species. Rondel-trapeziform short cell could have been observed

© The Author(s) 2015

Tab. 2 Distribution of phytolith morphotypes in the examined shoots of *Poa* species. N – code of morphotypes; Fig. – figure number; *n* – total; % – frequency in the classified phytolith assemblage of the nine species; ubiquity – presence of morphotypes in species.

N	Fig.	First descriptor	Second descriptor	prat (1)	ang (2)	alp (3)	stir (4)	ann (5)	arc (6)	comp (7)	hyb (8)	triv (9)	*n*	%	Presence in species	Ubiquity /9 species
	2–3	Elongate		440	103	41	231	76	215	354	174	167	1801	66.6	1 2 3 4 5 6 7 8 9	9
1	2a–b	Elongate	psilate	298	79	36	172	61	187	232	148	112	1325	49.0	1 2 3 4 5 6 7 8 9	9
2	2c	Elongate	sinuate	108	17	5	36	12	21	99	26	32	356	13.2	1 2 3 4 5 6 7 8 9	9
3	2d	Elongate	castelate	2			13			12		8	35	1.3	1 4 7 9	4
4	3a	Elongate	echinate	13	3		3	2	5			3	29	1.1	1 2 4 5 6 9	6
5	3b	Elongate	depressed psilate	7	2		2	1				2	14	0.5	1 2 4 5 9	5
6	3c	Elongate	crenate	2	1		3					5	11	0.4	1 2 4 9	4
7	3d	Elongate	papillate						1	7			8	0.3	6 7	2
8	3e	Elongate	granulate				1					5	6	0.2	4 9	2
9	3f	Elongate	verrucate	4						1			5	0.2	1 7	2
10	3g	Elongate	corniculate	2									2	0.1	1	1
11	3h	Elongate	lacunose	2						2			4	0.1	1 7	2
12	3i	Elongate	pilate	2			1			1			4	0.1	1 4 7	3
13	3j	Elongate	columellate						1				1	0.03	6	1
14	3k	Elongate	dendriform		1								1	0.03	2	1
15	4a	Oblong	psilate						1				1	0.03	6	1
16	4b	Rondel-trapeziform	psilate	277	145	7	3	18	53	16	36	6	561	20.7	1 2 3 4 5 6 7 8 9	9
17	4c	Globular inclusion	psilate			7			3	64			74	2.7	3 6 7	3
18	4d	Tabular	psilate	50	3				3	3	2	2	63	2.3	1 2 6 7 8 9	6
19	5a	Lanceolate trichome	psilate	23	3		1	3	6	9	11	2	58	2.1	1 2 4 5 6 7 8 9	8
20	5b–d	Bulliform	psilate	24								2	26	1.0	1 9	2
21	5e	Papilla	psilate	19									19	0.7	1	1
22	5f	Rectangle	psilate					3	3	10			16	0.6	5 6 7	3
23	5g	Stellate	laminate	4	2	2			1	2	5		16	0.6	1 2 3 6 7 8	6
24	5h	Square	psilate			9			1	4		2	16	0.6	3 6 7 9	4
25	5i	Trigonal pyramid	psilate	7	1				5				13	0.5	1 2 6	3

© The Author(s) 2015 Published by Polish Botanical Society

Tab. 2 *(continued)*

N	Fig.	First descriptor	Second descriptor	prat (1)	ang (2)	alp (3)	stir (4)	ann (5)	arc (6)	comp (7)	hyb (8)	triv (9)	*n*	%	Presence in species	Ubiquity /9 species
26	4c	Globular	psilate	3					12				15	0.5	1 6	2
27	5j	Scutiform	psilate	4	2							4	10	0.4	1 2 9	3
28	5k	Papilla with pitted edge								5			5	0.2	7	1
29	5l	Cubic	psilate	3				1				2	6	0.2	1 5 9	3
30	5m	Polylobate	psilate				1				1		2	0.1	4 8	2
31	5n	Bilobate	psilate	1									1	0.03	1	1
		Classified		855	259	66	236	101	303	467	229	187	2703	100		
		Unclassified		1243	161	331	82	305	679	395	109	215	3520			
		Classified %		40.7	61.6	16.6	74.2	24.8	30.8	54.1	67.7	46.5	43.4			

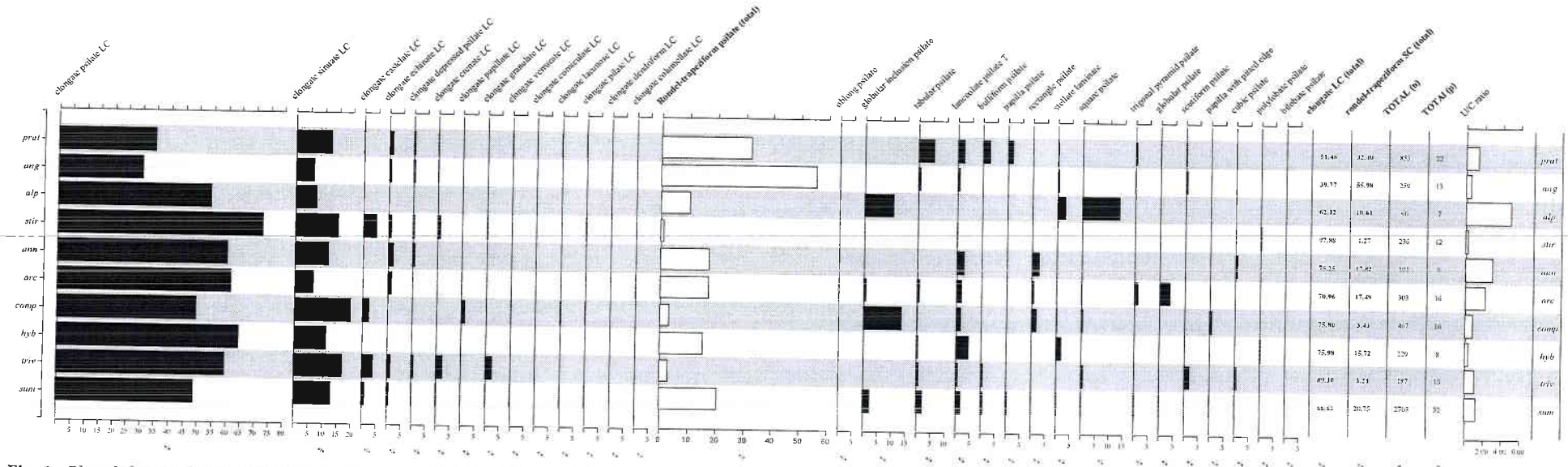

Fig. 1 Phytolith morphotype distribution in *Poa* species lateral shoots. LC – long cell; SC – short cell; T – trichome; U/C – unclassified/classified phytolith ratio; prat – *P. pratensis*; ang – *P. angustifolia*; alp – *P. alpigena*; stir – *P. stiriaca*; ann – *P. annua*; arc – *P. arctica*; comp – *P. compressa*; hyb – *P. hybrida*; triv – *P. trivialis*.

© The Author(s) 2015 Published by Polish Botanical Society Acta Soc Bot Pol 84(3):369–383

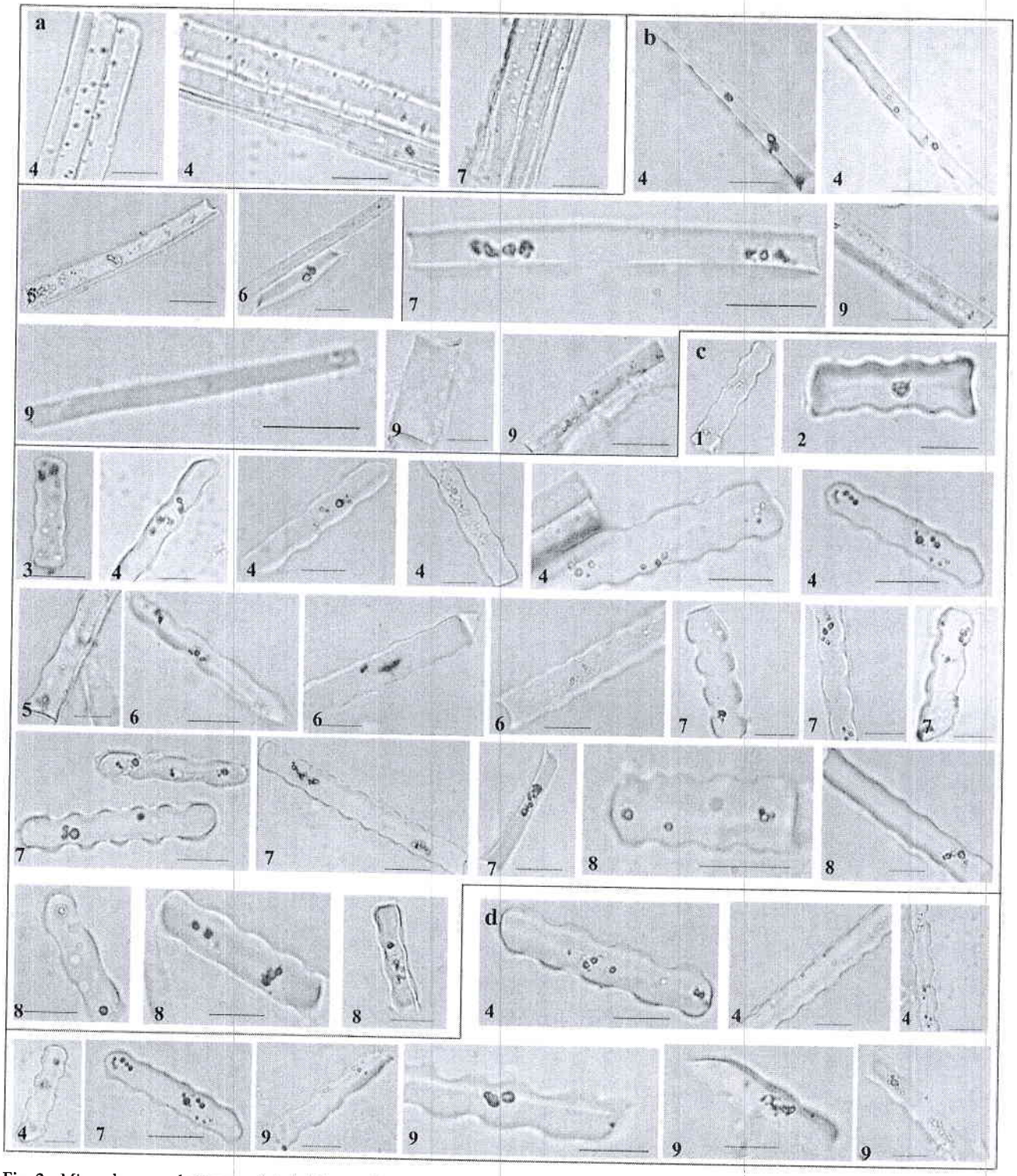

Fig. 2 Microphotograph images of phytolith morphotypes recovered from lateral shoots of *Poa* species. **a** Elongate psilate and scrobiculate (pitted) tracheary elements. **b** Elongate psilate epidermal long cells. **c** Elongate sinuate epidermal long cells. **d** Elongate castelate epidermal long cells. 1 – *P. pratensis*; 2 – *P. angustifolia*; 3 – *P. alpigena*; 4 – *P. stiriaca*; 5 – *P. annua*; 6 – *P. arctica*; 7 – *P. compressa*; 8 – *P. hybrida*; 9 – *P. trivialis*. Scale bars: 10 μm.

with different sizes in surfaces of *P. arctica* leaves (Fig. 8e,f). There are some silicified SC in the costal zone of abaxial epidermis of *P. annua* and *P. arctica* but it does not reach the number accordance with the abundant trichomes of silicified SC of *P. angustifolia* or *P. pratensis*. *Poa compressa* leaves characterized by less rondel-trapeziform SC and the most number globular inclusion phytoliths (Fig. 9a,b). Lanceolate was the dominant morphology in *P. hybrida*, which is in accordance with the abundant trichomes (Fig. 9c,d). There were lot of elongate LC with different ornaments in *P. trivialis*. As Fig. 9e,f shows, scutiforms – originated in unicellular hairs – were also common. *Poa hybrida* abaxial

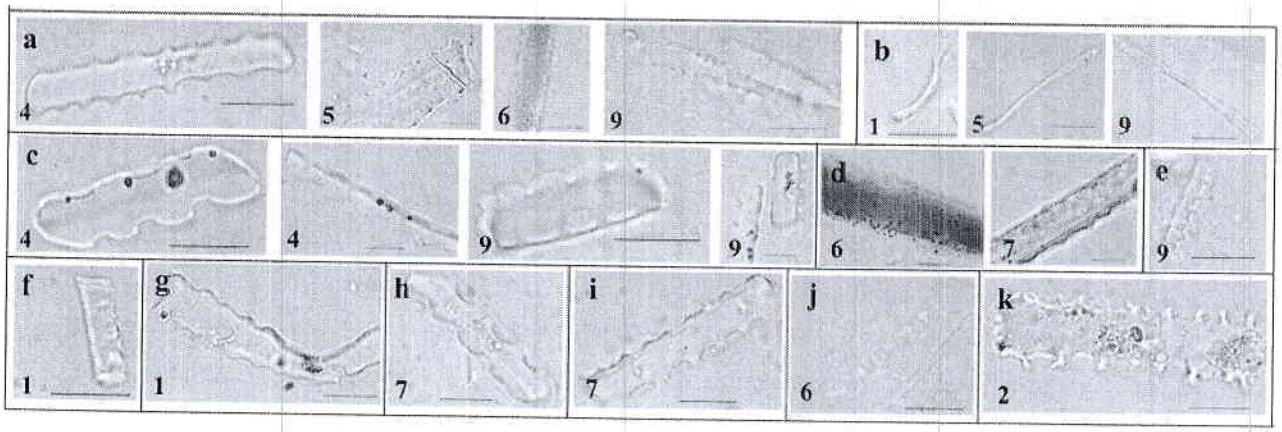

Fig. 3 Microphotograph images of phytolith morphotypes recovered from lateral shoots of *Poa* species. **a** Elongate echinate epidermal long cells. **b** Elongate psilate, depressed epidermal long cells. **c** Elongate crenate epidermal long cells. **d** Elongate papillate epidermal long cells. **e** Elongate granulate epidermal long cell. **f** Elongate verrucate epidermal long cell. **g** Elongate corniculate epidermal long cell. **h** Elongate lacunose epidermal long cell. **i** Elongate pilate epidermal long cell. **j** Elongate columellate epidermal long cell. **k** Elongate dendriform epidermal long cell. 1 – *P. pratensis*; 2 – *P. angustifolia*; 3 – *P. alpigena*; 4 – *P. stiriaca*; 5 – *P. annua*; 6 – *P. arctica*; 7 – *P. compressa*; 8 – *P. hybrida*; 9 – *P. trivialis*. Scale bars: 10 μm.

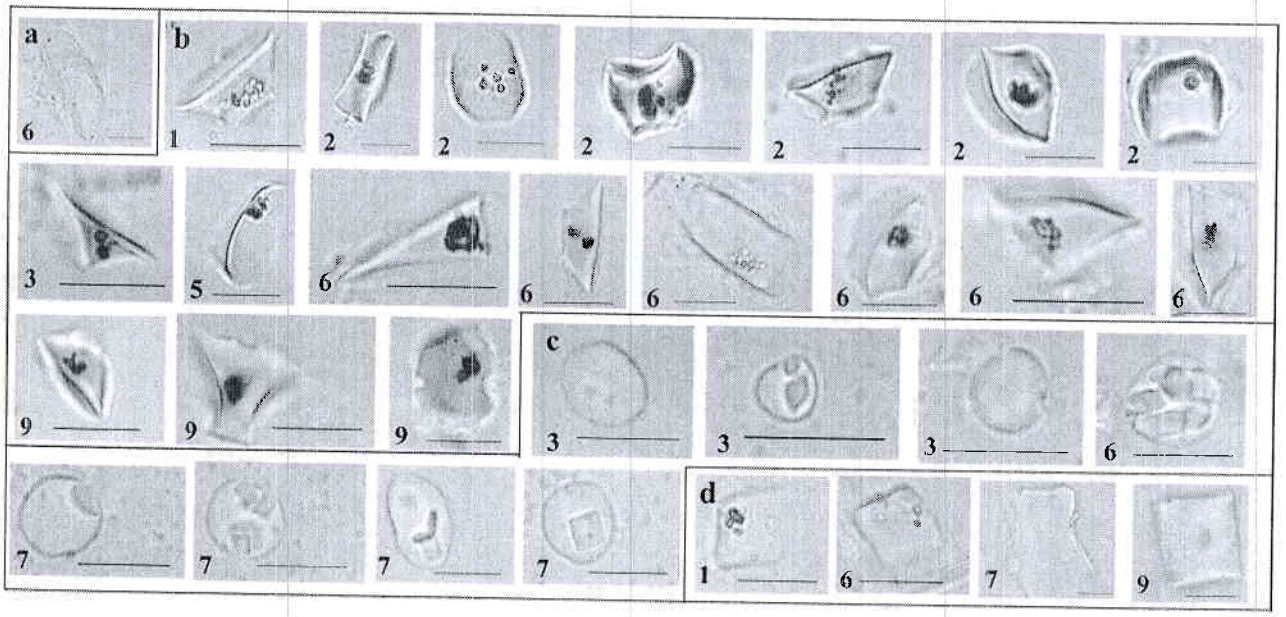

Fig. 4 Microphotpgraph images of phytolith morphotypes recovered from lateral shoots of *Poa* species. **a** Oblong psilate subepidermal cell. **b** Rondel-trapeziform epidermal short cells. **c** Globular psilate with inclusion subepidermal cells. **d** Tabular epidermal cells. 1 – *P. pratensis*; 2 – *P. angustifolia*; 3 – *P. alpigena*; 4 – *P. stiriaca*; 5 – *P. annua*; 6 – *P. arctica*; 7 – *P. compressa*; 8 – *P. hybrida*; 9 – *P. trivialis*. Scale bars: 10 μm.

epidermis produce more rondel-trapeziform SC than the *P. compressa* and *P. trivialis* does.

Cluster analysis revealed four main groups: group 1, consisting of *P. pratensis* and *P. angustifolia*; group 2, consisting of the other species belonging to the *P. pratensis* species group: *P. alpigena*, *P. stiriaca*, and *P. trivialis* (the latter species is not a member of the group); group 3, consisting of three species: *P. annua*, *P. arctica* and *P. hybrida*; and group 4, consisting of *P. compressa* (Fig. 10).

The two closely relative species in group 1, *P. pratensis* and *P. angustifolia*, were characterized by more rondel-trapeziforms SC phytoliths and fewer elongate psilate LC than in the other *Poa* species (Fig. 1). Although group 3 (*P. annua*, *P. arctica* and *P. hybrida*) produced abundant rondel-trapeziform phytoliths, the rondel-trapeziform content is about half that of group 1. At the same time group 3 had about twice as many elongate LC morphotypes than group 1 (Fig. 1).

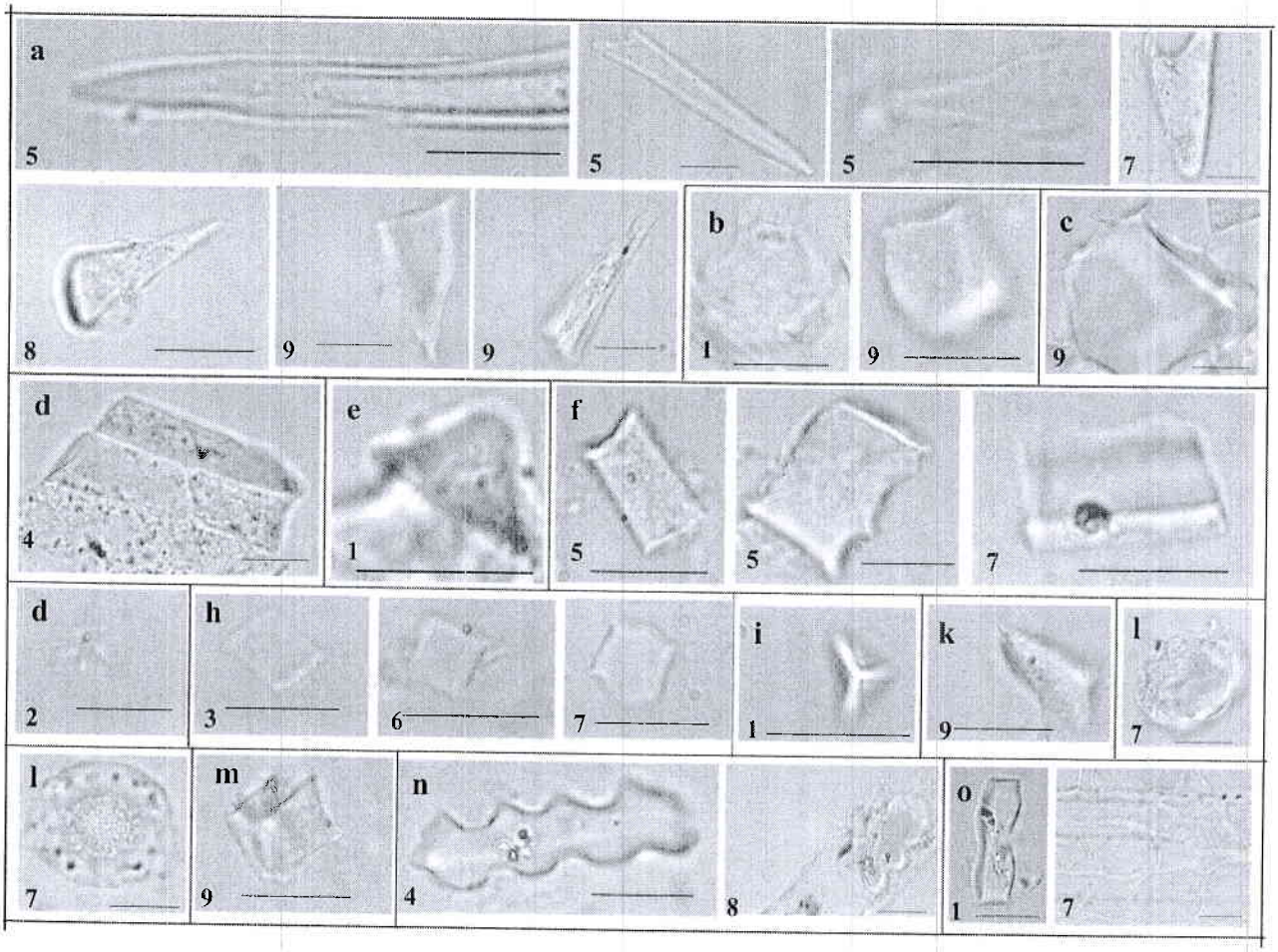

Fig. 5 Microphotpgraph images of phytolith morphotypes recovered from lateral shoots of *Poa* species. **a** Lanceolate trichome epidermal cells. **b** Cuneiform bulliform cells. **c** Blocky bulliform cell. **d** Bulliform cell group. **e** Papilla cell with base. **f** Rectangle epidermal cells. **g** Stellate laminate particular of cell wall. **h** Square silicic lamina from lumen of long cells. **i** Intercellular trigonal pyramid. **j** Scutiform psilate epidermal prickle. **k** Papilla with pitted edge. **l** Cubic epidermal short cell. **m** Plylobate epidermal long cells. **n** Bilobate epidermal long cell. **o** Subepidermal elements. 1 – *P. pratensis*; 2 – *P. angustifolia*; 3 – *P. alpigena*; 4 – *P. stiriaca*; 5 – *P. annua*; 6 – *P. arctica*; 7 – *P. compressa*; 8 – *P. hybrida*; 9 – *P. trivialis*. Scale bars: 10 μm.

The phytolith assemblage of *P. alpigena* was to a certain degree separated from the others in group 2. It is characterized by globular inclusion and square morphotypes. The phytolith assemblage of the two other species in group 2, *P. stiriaca* and *P. trivialis*, were similar to each other. Group 4 consisted of only *P. compressa*, which was characterized by globular inclusion phytoliths (Fig. 1).

The first two axes of the PCA (Fig. 11) amounted to 97.6% of the total variance (67.0% for axis 1, 30.5% for axis 2). On Fig. 11, where axes 1 and 2 are represented, two groups can be noted: group I: *P. pratensis* and *P. angustifolia*; species belonging to the *P. pratensis* species group); group II: other species belonging to the *P. pratensis* species group: *P. alpigena*, *P. stiriaca*, and the species that are not group members are *P. trivialis*, *P. annua*, *P. arctica* and *P. hybrida*, *P. compressa*. The morphotypes that mainly contribute to axis 1 are different types of elongate psilate phytoliths; rondel-trapeziform phytoliths contribute to axis 2. PCA of phytolith morphotypes confirms this observation (Fig. 12). Axes 1 and 2 are represented in Fig. 12, where axis 1 represents phytolith amount. The proportions of elongate sinuate and elongate psilate morphotypes are high in every species. Standard deviation of abundant rondel-trapeziform phytoliths are represented by axis 2. This morphotype is special because its proportion is high in every species but the standard deviation is higher than that of abundant elongate phytolith morphotypes.

Discussion

Compared to previously conducted studies on the biogenic silica content of *Poa* species, we can state that the biogenic silica content (16.8%) of the studied species is relatively high (cf. [28,37]), therefore it is anticipated that the *Poa* genus is present in fossil phytolith assemblages. *Poa pratensis* shoots (leaf blades and sheaths) accumulate silica mainly in their epidermis cells, both in short and long cells, as this feature is typical in most Poales [13,38]. There may be some connection between the bSi content and width of leaves of studied species because *Poa* specimens with wider leaves had lower bSi contents.

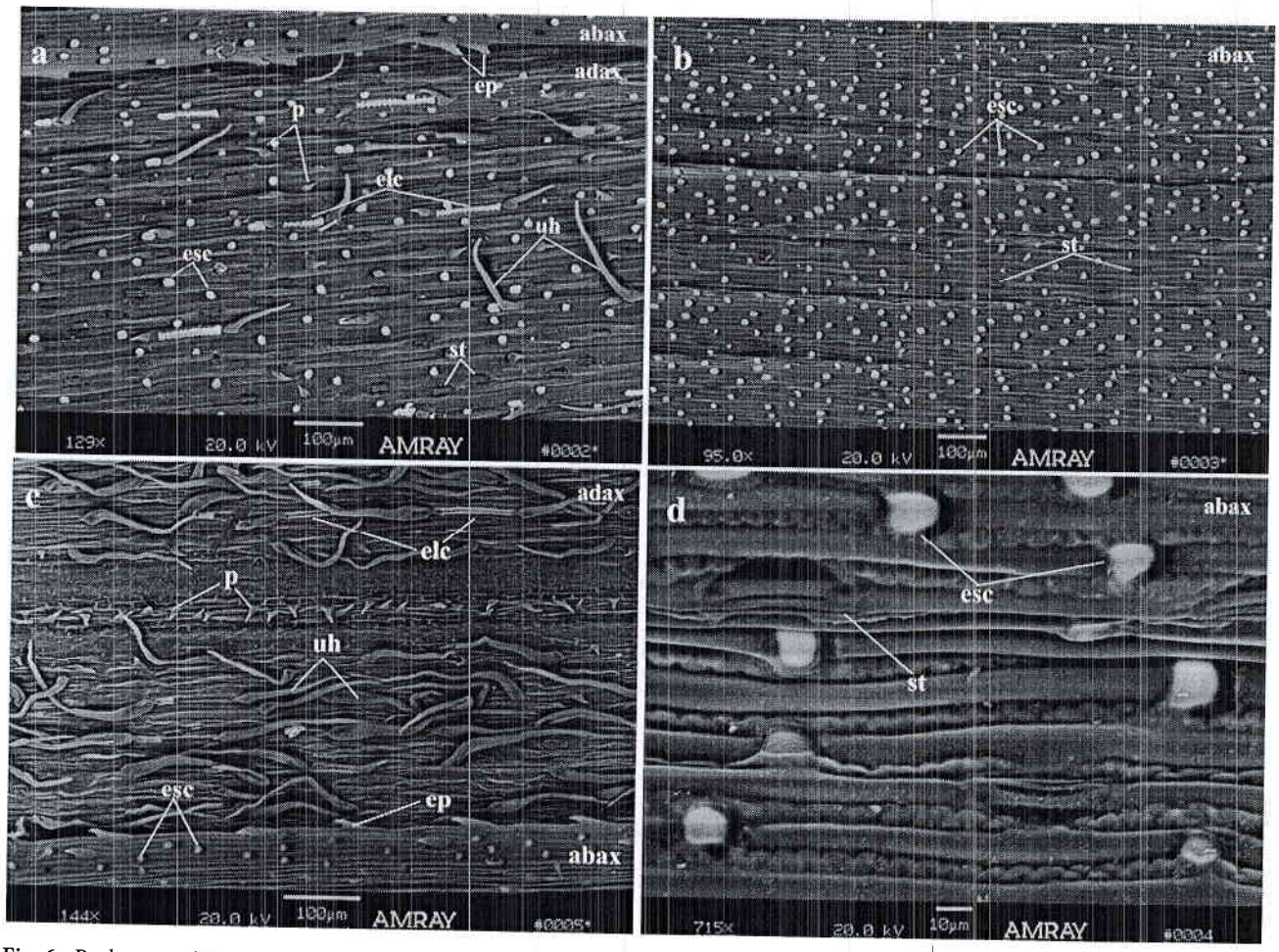

Fig. 6 Backscatter SEM images of lateral shoots of *Poa* species. **a** Adaxial leaf epidermis of *P. pratensis*. **b** Abaxial leaf epidermis of *P. pratensis*. **c** Adaxial leaf epidermis of *P. angustifolia*. **d** Abaxial leaf epidermis of *P. angustifolia*. abax – abaxial surface; adax – adaxial surface; elc – epidermal long cell; esc – epidermal short cell; ep – edge prickle; p – prickle; st – stomatal complex; uh – unicellular hair.

The phytolith assemblages of the nine *Poa* species are compounded by several morphotypes described previously for other species of the family [16], complemented by the two morphotypes found in *Poa* leaves by Lisztes-Szabó et al. [24]. The *Poa* genus (represented by the nine studied species) is characterized by elongate psilate, rondel-trapeziform phytoliths, and lanceolate or scutiform morphotypes (long, unicellular hairs and short prickles).

There is a diverse range of silica body morphologies in Poaceae, including dumbbell-shaped, cross-shaped intermediates between these two types, horizontally elongated shapes with psilate or sinuous outlines, saddle-shaped, conical-shaped and numerous others [13,38,39]. It is interesting to note that the cross-shaped and saddle-shaped forms were absent in the examined *Poa* shoots, similarly to Brown's results [4], and at the same time lobated phytoliths were not found, unlike in *Poa alpina* epidermis where this type is dominant [37]. Only a few prickles (unicellular trichomes), and especially the peak of them could be observed, because long, multicellular trichomes are not typical in this species [38]. However, it is also true that the silica content is higher in the apex of the prickles than in their base, therefore the recovery and observation of apex fragments has a higher probability.

Similarly to the study of Morris et al. [40], only scarce amounts of bulliforms were found. Nonetheless, strongly silicified bullifoms are frequently detected in the soil-phytolith assemblages of the geographical area of these species. It is likely that, the silification of the bulliforms are typical for the C4 species rather, than the C3 *Poa* species.

The results match and corroborate with the descriptions published by other authors, who noted the predominance of the same phytoliths morphologies: *P. secunda* ([40] – Great Basin, USA; [16] – Pacific Northwest, USA). The three-part division [3] seems to be relevant for the *Poa* genus because frequencies of saddle (typical of Panicoideae) and bilobate (typical of Chloridoideae) were low (only one lobate was found in this study), but circular/oval rectangular (in the present study: rondel-trapeziform) frequency was high (typical of Pooideae).

Having summarized our results regarding morphotype frequency, we supported the conclusion of Brown [4] and Marx et al. [41]. They argued that interspecific variations of phytolith morphotypes can be observed. Not all shapes common to a given species were found in each specimen. Genetic variation among plants and the geographical location where the plants grew may cause intraspecific differences in phytolith assemblages [42,43] and these may fix

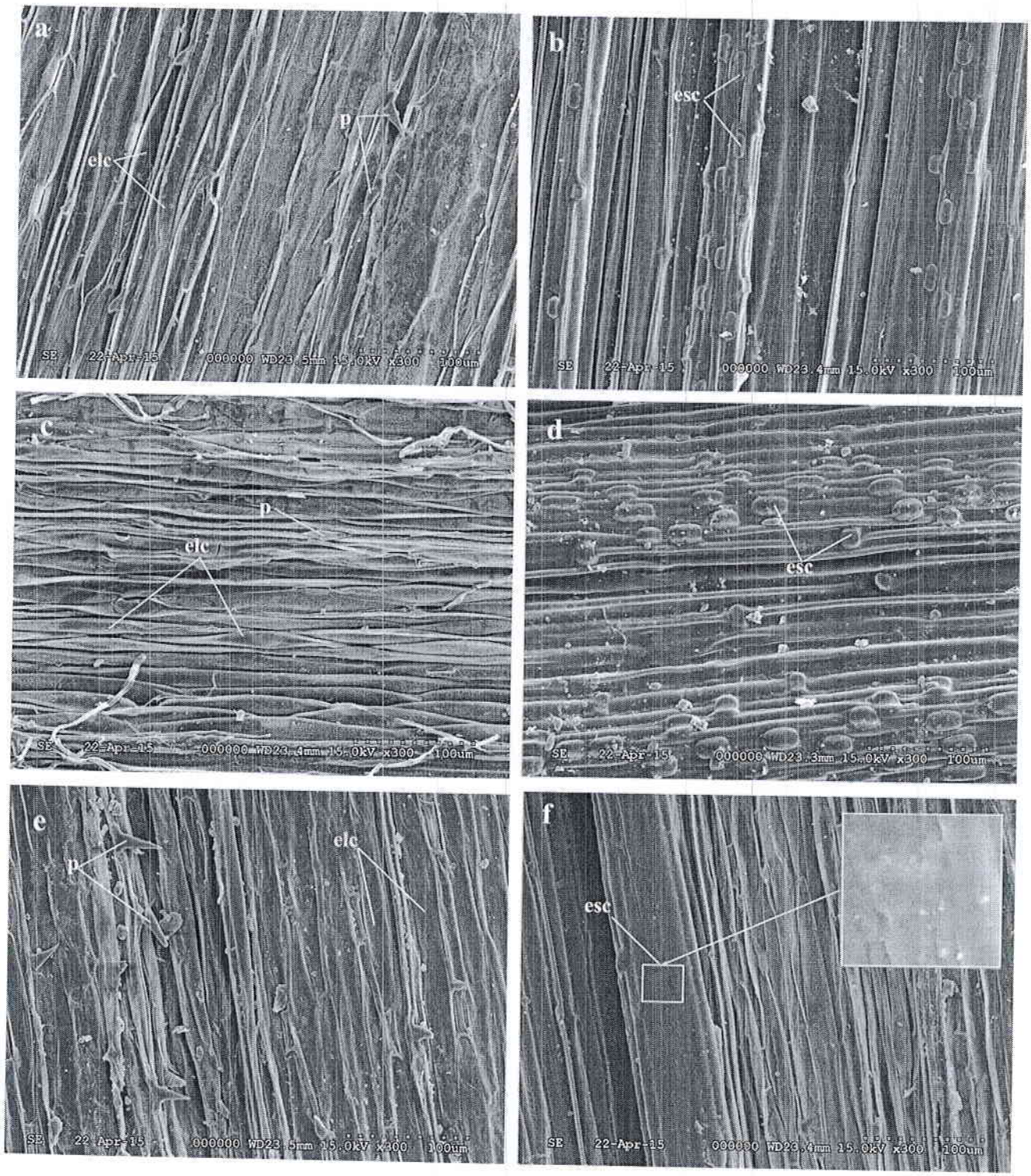

Fig. 7 SEM images of lateral shoots of *Poa* species. **a** Adaxial leaf epidermis of *P. pratensis*. **b** Abaxial leaf epidermis of *P. pratensis*. **c** Adaxial leaf epidermis of *P. angustifolia*. **d** Abaxial leaf epidermis of *P. angustifolia*. **e** Adaxial leaf epidermis of *P. alpigena*. **f** Abaxial leaf epidermis of *P. alpigena*. elc – epidermal long cell; esc – epidermal short cell; p – prickle; uh – unicellular hair.

at species level. The two closely relative *Poa* species of the *P. pratensis* species group, *P. pratensis* and *P. angustifolia*, slightly differ in the abundance of rondel-trapeziform SC phytoliths from those of the other *Poa* species. This result confirmed the previous taxonomic statements, because the phytolith that originate from SC are genetically fixed and have taxonomical relevance [44,45]. Blinnikov et al. [46] also identified several rondels and plates of blue meadow grass in grasslands of controlled composition on experimental plots (at Cedar Creek, Minnesota). Rondels (or truncated cones) have been assigned generally to the subfamily Pooideae. However, there are some pooid species (*Melica brasiliana*) that do not produce this morphotype, whereas species from other subfamilies produce them in great quantities (*Stipa*

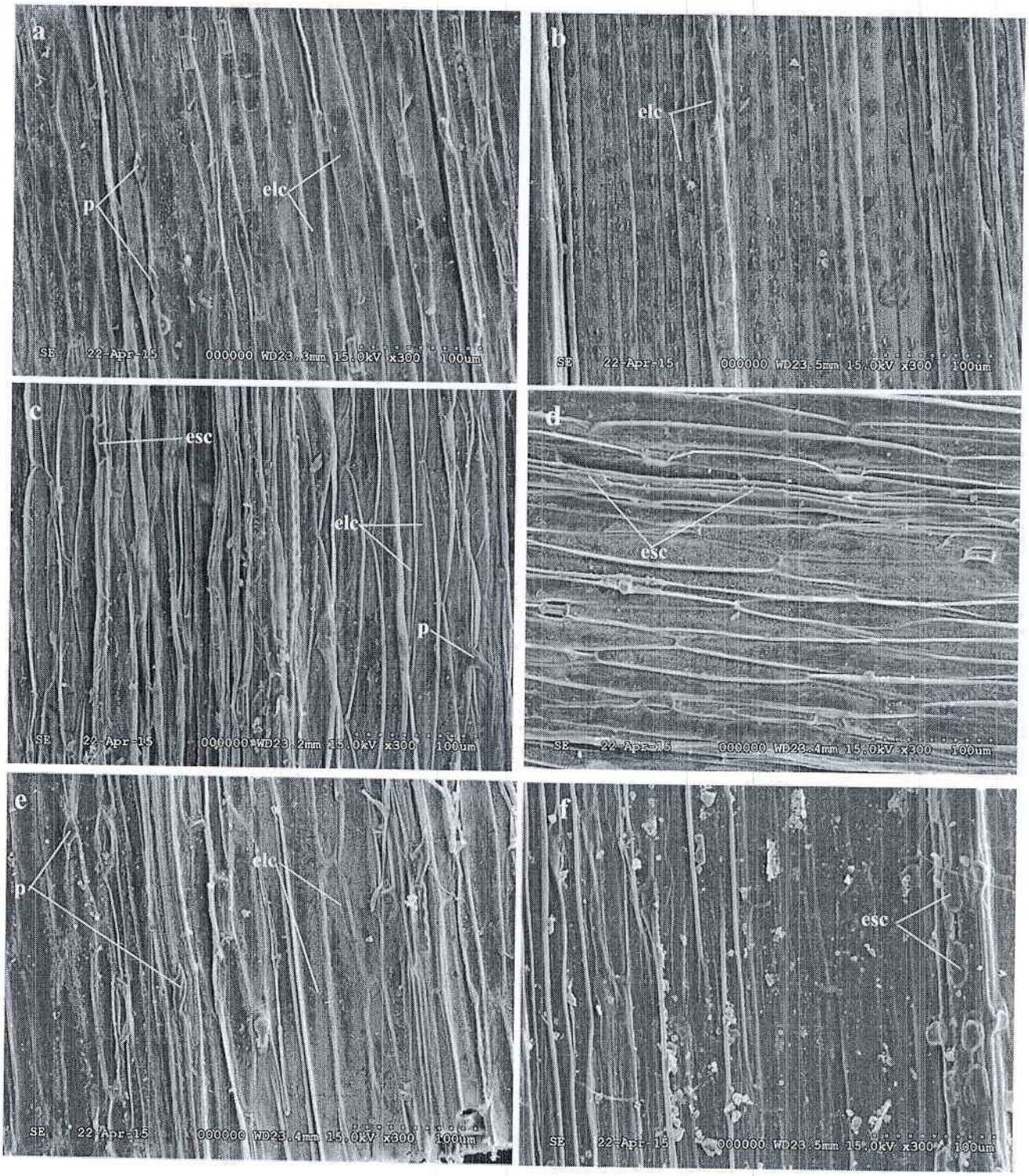

Fig. 8 SEM images of lateral shoots of *Poa* species. a Adaxial leaf epidermis of *P. stiriaca*. **b** Abaxial leaf epidermis of *P. stiriaca*. **c** Adaxial leaf epidermis of *P. annua*. **d** Abaxial leaf epidermis of *P. annua*. **e** Adaxial leaf epidermis of *P. arctica*. **f** Abaxial leaf epidermis of *P. arctica*. elc – epidermal long cell; esc – epidermal short cell; p – prickle; st – stomatal complex; uh – unicellular hair.

spp. and *Piptochaetium* spp.). Barboni and Bremond [47] studied 184 East-African grass species and found that there are morphological variations (of size and number of lobes) within the rondels, which could additionally be considered to improve environmental and taxonomical interpretation of phytolith assemblages.

Similar establishment was reported for palms, because it was not possible to identify unambiguously to taxon individual palm phytoliths. Interspecific differences in phytolith morphology significantly outweighed intraspecific variation, revealing the potential value of further research [48]. Thorn [49] compared phytolith assemblage of *P. litoralis* with those

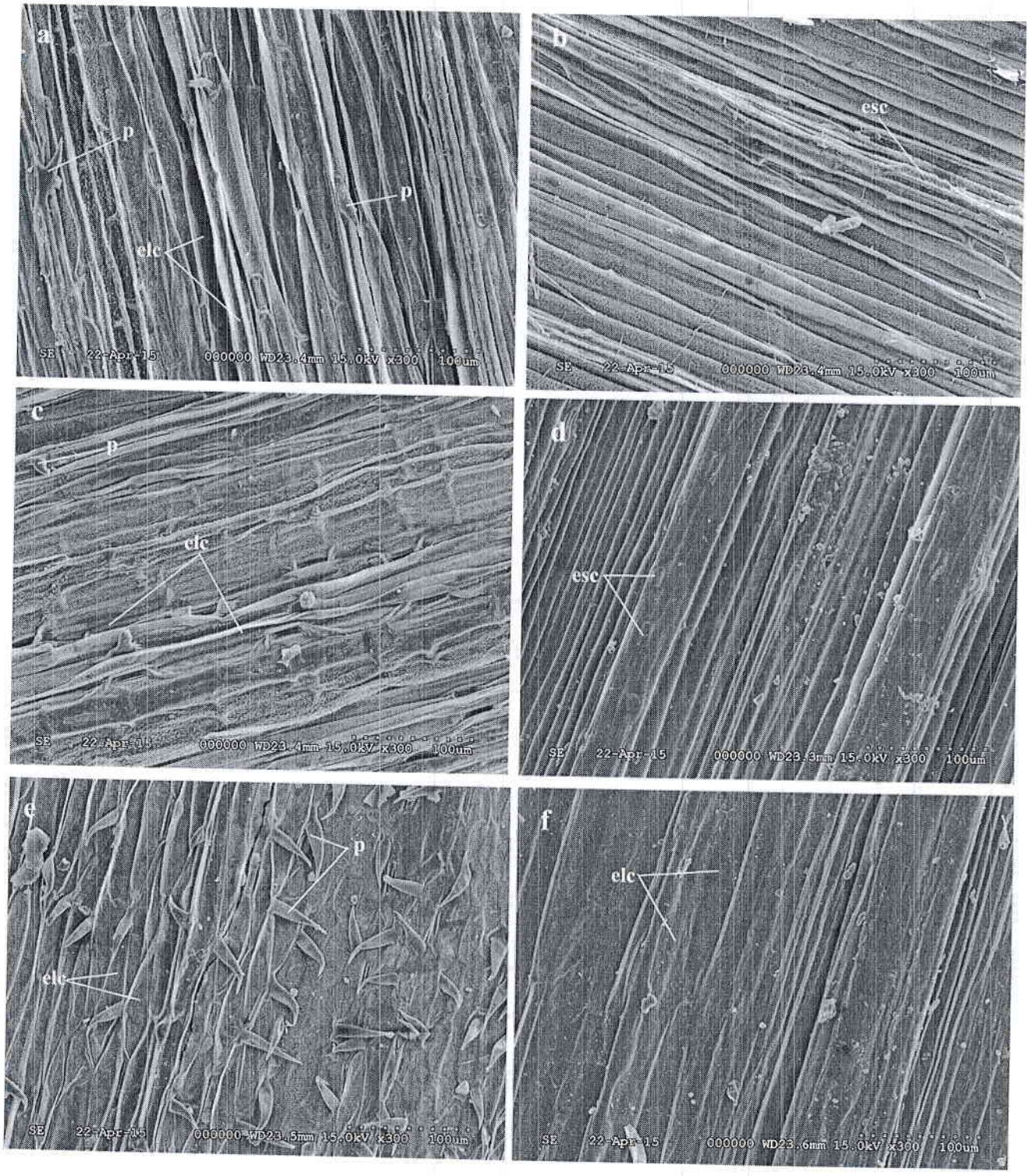

Fig. 9 SEM images of lateral shoots of *Poa* species. **a** Adaxial leaf epidermis of *P. compressa*. **b** Abaxial leaf epidermis of *P. compressa*. **c** Adaxial leaf epidermis of *P. hybrida*. **d** Abaxial leaf epidermis of *P. hybrida*. **e** Adaxial leaf epidermis of *P. trivialis*. **f** Abaxial leaf epidermis of *P. trivialis*. elc – epidermal long cell; esc – epidermal short cell; p – prickle; st – stomatal complex.

of an unidentified *Poa* species and reported about the variation within the *Poa* at the generic level.

The cluster analysis and PCA reflect quite clearly the systematics of the group of species under study. Firstly, it is possible to distinguish between the two groups analyzed: *P. pratensis* agg. and other *Poa* species. The differences lie in the phytolith morphotypes. As Shaheen et al. [50] found in the genus *Brachiaria*, and subsequent upon our *Poa* study the quantitative analysis of phytoliths may provide a new taxonomic character to distinguish different species of a grass genus.

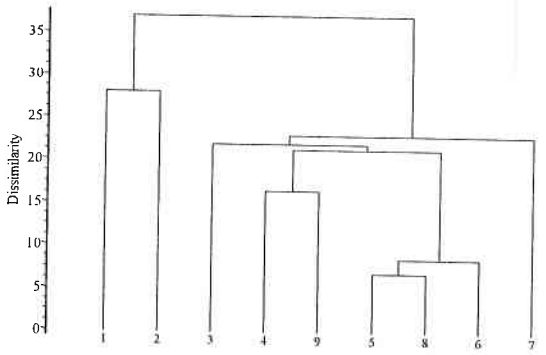

Fig. 10 Hierarchical cluster dendrogram showing *Poa* species grouping based on their phytolith assemblages (single link, nearest neighbour). Species: 1 – *P. pratensis*; 2 – *P. angustifolia*; 3 – *P. alpigena*; 4 – *P. stiriaca*; 5 – *P. annua*; 6 – *P. arctica*; 7 – *P. compressa*; 8 – *P. hybrida*; 9 – *P. trivialis*.

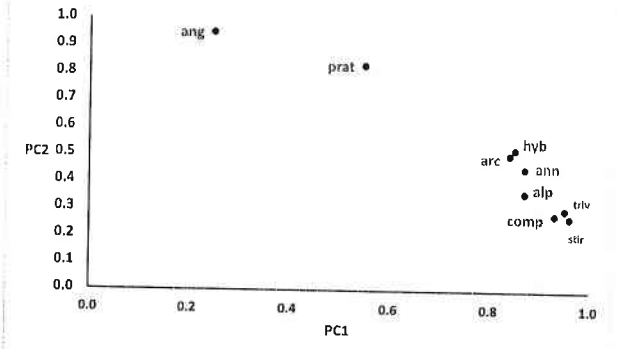

Fig. 11 Principal component analysis axes score plot of species based on their phytolith assemblages.

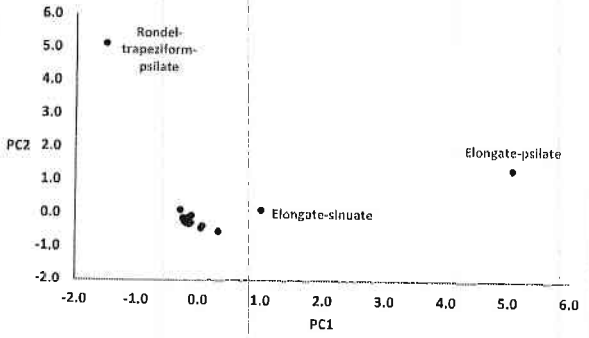

Fig. 12 Principal component analysis axes score plot of phytolith morphotypes.

Conclusions

This description of leaf phytolith assemblages of *P. pratensis*, *P. angustifolia*, *P. alpigena*, *P. stiriaca*, *P. trivialis*, *P. annua*, *P. arctica*, *P. hybrida* and *P. compressa* represents the first contribution for nine different species in the same genus. Since *Poa* species are characterized by diverse geographical distributions it is proposed that their phytoliths are of significant value in ecological studies. Finally, some characters of phytolith assemblages are described to allow the collection of reference material to start in order to compare other grass species and genera in the grasslands of the Northern Hemisphere in the future. Although our results do match the general patterns of phytolith assemblages within a grass subfamily as described by other authors, it is necessary to consider the exceptions found here, especially when linking the relative frequencies of morphologies to plant systematics.

Acknowledgments

The authors would like to thank Ibolya O. Tóth and Hanga Kiss for technical assistance. The authors are also grateful to two anonymous reviewers whose comments helped to improve this paper. This work was undertaken with the support of Department of Agricultural Botany, Crop Physiology and Biotechnology (University of Debrecen) and Research Centre of Excellence at Szent István University (9878/2015/FEKUT).

Authors' contributions

The following declarations about authors' contributions to the research have been made: writing the manuscript: ZLS; conducting measurements: SK; statistical analysis: PB; conducting SEM studies: LD; revising of taxonomic consequences: KP; research designing: ÁP.

Competing interests

No competing interests have been declared.

References

1. Blackman E, Parry DW. Opaline silica bodies in the range grasses of southern Alberta. Can J Bot. 1968;49(5):769–781. http://dx.doi.org/10.1139/b71-116
2. Agarie S, Agata W, Uchida H, Kubota F, Kaufman P. Function of silica bodies in the epidermal system of rice (*Oryza sativa* L.): testing the window hypothesis. J Exp Bot. 1996;47(5):655–660. http://dx.doi.org/10.1093/jxb/47.5.655
3. Twiss PC, Suess E, Smith RM. Morphological classification of grass phytoliths. Soil Sci Soc Am J. 1969;33(1):109–115. http://dx.doi.org/10.2136/sssaj1969.03615995003300010030x
4. Brown DA. Prospects and limits of a phytolith key for grasses in the Central United States. J Archaeol Sci. 1984;11(4):345–368. http://dx.doi.org/10.1016/0305-4403(84)90016-5
5. Mulholland SC. Phytolith shape frequencies in North Dakota grasses: a comparison to general patterns. J Archaeol Sci. 1989;16(5):489–511. http://dx.doi.org/10.1016/0305-4403(89)90070-8
6. Mulholland SC, Rapp G. A morphological classification of grass silica bodies. In: Rapp G, Mulholland SC, editors. Phytolith systematics. New York, NY: Plenum Press; 1992. p. 65–89. http://dx.doi.org/10.1007/978-1-4899-1155-1_4
7. Fredlund GG, Tieszen LT. Modern phytolith assemblages from the North American Great Plains. J Biogeogr. 1994;21(3):312–335. http://dx.doi.org/10.2307/2845533
8. Twiss PC. Predicted world distribution of C3 and C4 grass phytoliths. In: Rapp G, Mulholland SC, editors. Phytolith systematics. New York, NY: Plenum Press; 1992. p. 113–128. http://dx.doi.org/10.1007/978-1-4899-1155-1_6
9. Lindstrom LI, Boo BM, Mujica MB, Lutz EE. Silica bodies in perennial grasses of the southern District of the Calden in central Argentina. Phyton. 2000;69:127–135.
10. Mejia-Saules T, Bisby FA. Silica bodies and hooked papillae in lemmas of *Melica* species (Gramineae: Pooideae). Bot J Lin Soc. 2003;141(4):447–463. http://dx.doi.org/10.1046/j.1095-8339.2003.00152.x
11. Krishnan S, Samson NP, Ravichandran P, Narasimhan D,

Dayanandan P. Phytoliths of Indian grasses and their potential use in identification. Bot J Lin Soc. 2000;132(3):241–252. http://dx.doi.org/10.1111/j.1095-8339.2000.tb01529.x

12. Lu H, Liu KB. Morphological variations of lobate phytoliths from grasses in China and the south-eastern United States. Divers Distrib. 2003;9(1):73–87. http://dx.doi.org/10.1046/j.1472-4642.2003.00166.x

13. Prychid CJ, Rudall PJ, Gregory M. Systematics and biology of silica bodies in monocotyledons. Bot Rev. 2004;69(4):377–440. http://dx.doi.org/10.1663/0006-8101(2004)069[0377:SABOSB]2.0.CO;2

14. Clayton WD, Renvoize SA, editors. Genera graminum: grasses of the world. London: Royal Botanic Gardens; 1986. (Kew Bulletin Additional Series; vol 13).

15. Soó R. A Magyar flóra és vegetáció rendszertani – növényföldrajzi kézikönyve V. 2nd ed. Budapest: Akadémiai Kiadó; 1973.

16. Blinnikov MS. Phytoliths in plants and soils of the interior Pacific Northwest, USA. Rev Palaeobot Palynol. 2005;135(1–2):71–98. http://dx.doi.org/10.1016/j.revpalbo.2005.02.006

17. de Melo SP, Monteiro FA, de Bona FD. Silicon distribution and accumulation in shoot tissue of the tropical forage grass *Brachiaria brizantha*. Plant Soil. 2010;336(1–2):241–249. http://dx.doi.org/10.1007/s11104-010-0472-5

18. Hartley W. Studies on the origin, evolution, and distribution of the Gramineae. IV. The genus *Poa* L. Aust J Bot. 1961;9(2):152–161. http://dx.doi.org/10.1071/bt9610152

19. Blinnikov MS, Busacca A, Whitlock C. Reconstruction of the late Pleistocene grassland of the Columbia basin, Washington, USA, based on phytolith records in loess. Palaeogeogr Palaeoclimatol Palaeoecol. 2002;177(1–2):77–101. http://dx.doi.org/10.1016/s0031-0182(01)00353-4

20. Tutin TG, Heywood VH, Burges NA, Moore DM, Valentine DH, Walters SM, et al. Flora Europaea. Volume 5. Cambridge: Cambridge University Press; 1980.

21. Chaffey NJ. Epidermal structure in the ligules of four species of the genus *Poa* L. (Poaceae). Bot J Lin Soc. 1984;89(4):341–354. http://dx.doi.org/10.1111/j.1095-8339.1984.tb02565.x

22. Chaffey NJ. Structure and function in the grass ligule: presence of veined and membranous ligules on the same culm of British grasses. New Phytol. 1985;101(4):613–621. http://dx.doi.org/10.1111/j.1469-8137.1985.tb02867.x

23. Szabó KZ, Papp M, Daróczi L. Ligule morphology and anatomy of five Poa species. Acta Biol Crac Ser Bot. 2006;48(2):83–88.

24. Lisztes-Szabó Z, Kovács S, Pető Á. Phytolith analysis of *Poa pratensis* (Poaceae) leaves. Turk J Bot. 2014;38(1):851–863. http://dx.doi.org/10.3906/bot-1311-8

25. Matzk F. New efforts to overcome apomixis in *Poa pratensis*. Euphytica. 1991;55(1):65–72. http://dx.doi.org/10.1007/bf00022561

26. USDA, NRCS. The PLANTS Database [Internet]. Greensboro, NC: National Plant Data Team; 2014 [cited 2009 Aug 18]; Available from: http://plants.usda.gov

27. Albert RM, Weiner S. Study of opal phytoliths in prehistoric ash layers using a quantitative approach. In: Meunier J, Coline F, editors. Phytoliths: applications in earth sciences and human history. Lisse: Balkema; 2001. p. 251–266.

28. Mercader J, Astudillo F, Barkworth M, Bennett T, Esselmont C, Kinyanjui R, et al. Poaceae phytoliths from Niassa Rift, Mozambique. J Archaeol Sci. 2010;37(8):1953–1967. http://dx.doi.org/10.1016/j.jas.2010.03.001

29. Mercader J, Bennett T, Esselmont C, Simpson S, Walde D. Phytoliths in woody plants from the Miombo woodlands of Mozambique. Ann Bot. 2009;104(1):91–113. http://dx.doi.org/10.1093/aob/mcp097

30. Madella M, Alexandre A, Ball T. International Code for Phytolith Nomenclature 1.0. Ann Bot. 2005;96(2):253–260. http://dx.doi.org/10.1093/aob/mci172

31. Blinnikov MS, Gaglioti BV, Walker DA, Wooller MJ, Zazula GD. Pleistocene graminoid-dominated ecosystems in the Arctic. Quat Sci Rev. 2011;30(21–22):2906–2929. http://dx.doi.org/10.1016/j.quascirev.2011.07.002

32. Honaine MF, Osterrieth ML. Silification of the adaxial epidermis of leaves of panicoid grass in relation to leaf position and section and environmental conditions. Plant Biol. 2012;14(4):596–604. http://dx.doi.org/10.1111/j.1438-8677.2011.00530.x

33. Yost CL, Blinnikov MS. Locally diagnostic phytoliths of wild rice (*Zizania palustris* L.) from Minnesota, USA: comparison to other wetland grasses and usefulness for archaeobotany and paleoecological reconstructions. J Archaeol Sci. 2011;38(8):1977–1991. http://dx.doi.org/10.1016/j.jas.2011.04.016

34. Piperno DR, Pearsall DM. The silica bodies of tropical American grasses: morphology, taxonomy, and implications for grass systematics and fossil phytolith identification. Washington, DC: Smithsonian Institution Scholarly Press; 1998. (Smithsonian Contributions to Botany; vol 85). http://dx.doi.org/10.5479/si.0081024x.85

35. Juggins S. C2 version 1.5 user guide. Software for ecological and palaeoecological data analysis and visualisation. Newcastle upon Tyne: Newcastle University; 2007.

36. Jolliffe IT. Principal component analysis. New York, NY: Springer-Verlag; 2002.

37. Carnelli AL, Theurillat JP, Madella M. Phytolith types and type-frequencies in subalpine–alpine plant species of the European Alps. Rev Palaeobot Palynol. 2004;129(1–2):39–65. http://dx.doi.org/10.1016/j.revpalbo.2003.11.002

38. Metcalfe CR. Anatomy of the monocotyledons I. Gramineae. Oxford: Clarendon Press; 1960.

39. Ponzi R, Pizzolongo P. Morphology and distribution of epidermal phytoliths in *Triticum aestivum* L. Plant Biosyst. 2003;137(1):3–10. http://dx.doi.org/10.1080/11263500312331351271

40. Morris LR, Baker FA, Morris C, Ryel RJ. Phytolith types and type-frequencies in native and introduced species of the sagebrush steppe and pinyon-juniper woodlands of the Great Basin, USA. Rev Palaeobot Palynol. 2009;157:339–357. http://dx.doi.org/10.1016/j.revpalbo.2009.06.007

41. Marx R, Lee DE, Lloyd KM, Lee WG. Phytolith morphology and biogenic silica concentrations and abundance in leaves of *Chionochloa* (Danthonieae) and *Festuca* (Poeae) in New Zealand. NZ J Bot. 2004;42(4):677–691. http://dx.doi.org/10.1080/0028825x.2004.9512919

42. Mulholland SC, Rapp G, Ollendorf AL, Regal R. Variation in phytoliths within a population of corn (Mandan Yellow Flour). Can J Bot. 1990;68(8):1638–1645. http://dx.doi.org/10.1139/b90-210

43. Mulholland SC, Rapp G, Ollendorf AL. Variation in phytoliths from corn leaves. Can J Bot. 1988;66:2001–2008.

44. Madella M, Lancelotti C, Osterrieth M. Comprehensive perspectives on phytolith studies in Quaternary research. Quat Int. 2012;287(1):1–2. http://dx.doi.org/10.1016/j.quaint.2012.11.009

45. Dani M, Farkas Á, Cseke K, Filep R, Kovács A. Leaf epidermal characteristics and genetic variability in Central European populations of broad-leaved *Festuca* L. taxa. Plant Syst Evol. 2014;300(3):431–451. http://dx.doi.org/10.1007/s00606-013-0893-8

46. Blinnikov MS, Bagent CM, Reyerson PE. Phytolith assemblages and opal concentrations from modern soils differentiate temperate grasslands of controlled composition on experimental plots at Cedar Creek, Minnesota. Quat Int. 2013;287:101–113. http://dx.doi.org/10.1016/j.quaint.2011.12.023

47. Barboni D, Bremond L. Phytoliths of East African grasses: an assessment of their environmental and taxonomic significance based on floristic data. Rev Palaeobot Palynol. 2009;158(1–2):29–41. http://dx.doi.org/10.1016/j.revpalbo.2009.07.002

48. Fenwick RSH, Lentfer CJ, Weisler MI. Palm reading: a pilot study to discriminate phytoliths of four Arecaceae (Palmae) taxa. J Archaeol Sci. 2011;38(9):2190–2199. http://dx.doi.org/10.1016/j.jas.2011.03.016

49. Thorn VC. Phytoliths from subantarctic Campbell Island: plant production and soil surface spectra. Rev Palaeobot Palynol. 2004;132(1-2):37–59. http://dx.doi.org/10.1016/j.revpalbo.2004.04.003

50. Shaheen S, Ahmad M, Khan F, Zafar M, Khan MA, Bano A, et al. Micormorphological diversity in leaf epidermal anatomy of *Brachiaria* species using elemental dispersive spectrophotometer analysis. J Med Plant Res. 2011;5:4279–4286.

51. Aiken SG, Dallwitz MJ, Consaul LL, McJannet CL, Boles RL, Argus GW, et al. Flora of the Canadian Arctic Archipelago: descriptions, illustrations, identification, and information retrieval [Internet]. Ottawa: NRC Research Press, National Research Council of Canada; 2007 [cited 2014 Aug 18]; Available from: http://nature.ca/aaflora/data